Cell Metabolism
Article

Pancreatic Polypeptide Controls Energy Homeostasis via *Npy6r* Signaling in the Suprachiasmatic Nucleus in Mice

Ernie Yulyaningsih,[1,5] Kim Loh,[1,5] Shu Lin,[1,5] Jackie Lau,[1] Lei Zhang,[1] Yanchuan Shi,[1] Britt A. Berning,[1] Ronaldo Enriquez,[1] Frank Driessler,[1] Laurence Macia,[1] Ee Cheng Khor,[1] Yue Qi,[1] Paul Baldock,[1] Amanda Sainsbury,[1,2,4,6] and Herbert Herzog[1,3,6,*]

[1]Neuroscience Program, Garvan Institute of Medical Research, St. Vincent's Hospital, 384 Victoria Street, Darlinghurst, Sydney NSW 2010, Australia
[2]School of Medical Sciences, Wallace Wurth Building, University of NSW, Botany Street, Sydney 2052, Australia
[3]UNSW Medicine, ASGM Building, University of NSW, Botany Street, Sydney 2052, Australia
[4]The Boden Institute of Obesity, Nutrition, Exercise, and Eating Disorders, Sydney Medical School, The University of Sydney, Medical Foundation Building, 92-94 Parramatta Road, Camperdown NSW 2006, Australia
[5]These authors contributed equally to this work
[6]Co-senior authors
*Correspondence: h.herzog@garvan.org.au
http://dx.doi.org/10.1016/j.cmet.2013.11.019

SUMMARY

Y-receptors control energy homeostasis, but the role of *Npy6* receptors (*Npy6r*) is largely unknown. Young *Npy6r*-deficient ($Npy6r^{-/-}$) mice have reduced body weight, lean mass, and adiposity, while older and high-fat-fed $Npy6r^{-/-}$ mice have low lean mass with increased adiposity. $Npy6r^{-/-}$ mice showed reduced hypothalamic growth hormone releasing hormone (*Ghrh*) expression and serum insulin-like growth factor-1 (IGF-1) levels relative to WT. This is likely due to impaired vasoactive intestinal peptide (VIP) signaling in the suprachiasmatic nucleus (SCN), where we found *Npy6r* coexpressed in VIP neurons. Peripheral administration of pancreatic polypeptide (PP) increased Fos expression in the SCN, increased energy expenditure, and reduced food intake in WT, but not $Npy6r^{-/-}$, mice. Moreover, intraperitoneal (i.p.) PP injection increased hypothalamic *Ghrh* mRNA expression and serum IGF-1 levels in WT, but not $Npy6r^{-/-}$, mice, an effect blocked by intracerebroventricular (i.c.v.) Vasoactive Intestinal Peptide (VPAC) receptors antagonism. Thus, PP-initiated signaling through *Npy6r* in VIP neurons regulates the growth hormone axis and body composition.

INTRODUCTION

Hypothalamic circuitries are important in receiving and integrating information from other brain areas as well as the periphery to control appetite and energy homeostasis (Sainsbury et al., 2002a). Among the many systems involved that influence orexigenic and anorexigenic processes in the hypothalamus, the neuropeptide Y (NPY) system is unique in that its major neuronal component, NPY, stimulates appetite and reduces energy expenditure, whereas its other family members, peptide YY (PYY) and pancreatic polypeptide (PP), which are mainly produced by endocrine cells in the periphery in response to food intake, act in an opposing fashion as satiety factors (Nguyen et al., 2011; Zhang et al., 2011). All three peptides are able to signal through a set of five known Y-receptors (*Npy1r*, *Npy2r*, *Ppyr1*, *Npy5r*, and *Npy6r*) for which they have different affinities (Nguyen et al., 2011; Zhang et al., 2011). It has now been well established through work with transgenic and knockout mouse models that *Npy1r* and *Npy5r* are mostly responsible for the appetite-stimulatory and energy-expenditure-related aspects of NPY signaling in the hypothalamus (Nguyen et al., 2012), whereas the *Npy2r* and *Ppyr1* are more critical for mediating satiety and other related aspects (Lin et al., 2009; Sainsbury et al., 2002b; Shi et al., 2010; Zhang et al., 2010). However, despite the large amount of work being dedicated to unraveling functions of the NPY system in the regulation of energy homeostasis, no information is available for the role of the *Npy6r*.

The *Npy6r* gene is less conserved than the other Y-receptors. It exists only as a truncated version in primate species, including humans (Gregor et al., 1996; Matsumoto et al., 1996; Rose et al., 1997), and it is absent from the rat genome (Burkhoff et al., 1998). The human *Npy6r* gene is located on chromosome 5q31 (Gregor et al., 1996) and contains a single-base deletion resulting in a frameshift mutation and an early stop codon (Gregor et al., 1996; Matsumoto et al., 1996; Rose et al., 1997). Interestingly, an alternative splice variant of the *Npy1r* has been discovered in the mouse leading to a truncated isoform of the protein similar to the human *Npy6r* (Nakamura et al., 1995), suggesting a potential for altered signaling capacity by *Npy1r*. Importantly, mRNA for the truncated *Npy1r* and the *Npy6r* is produced in considerable amounts, and in the case of the human *Npy6r*, mRNA is produced in the heart, skeletal muscle, gastrointestinal tissues, and adrenal glands as well as in the brain (Burkhoff et al., 1998; Gregor et al., 1996; Matsumoto et al., 1996), raising questions as to its possible function.

In contrast to humans, primates, and rats, the *Npy6r* gene is present in a nontruncated form in mice and rabbits (Burkhoff et al., 1998; Matsumoto et al., 1996). In the mouse, *Npy6r* is expressed in the developing embryo, skeletal muscle, kidney, and

testes (Burkhoff et al., 1998; Gregor et al., 1996). More importantly, in situ hybridization confirmed *Npy6r* expression in the mouse hypothalamus (Weinberg et al., 1996), suggesting a role for this receptor in the regulation of energy homeostasis. Controversy surrounds the pharmacological profile of the *Npy6r*, with some studies claiming an *Npy1r*-like profile (Weinberg et al., 1996), others indicating a *Ppyr1*-like profile (Gregor et al., 1996), and a further study describing a unique pharmacological profile of *Npy6r* distinct from all the other Y receptors (Mullins et al., 2000). This lack of consistent results arising from previous in vitro studies makes it difficult to ascertain the true pharmacology and potential physiological role of *Npy6r*.

Considering that mice are frequently used to determine the functional role of individual Y receptors, as well as the possibility that manipulation of the NPY system could be used for the development of new therapeutics for the treatment of obesity, diabetes, and related disorders, it is important to evaluate the contribution of all Y-receptors to the regulation of energy homeostasis, including *Npy6r* in the mouse. Therefore, in this study we investigated the metabolic characteristics and hypothalamic circuits activated by *Npy6r* signaling using *Npy6r* knockout mice ($Npy6r^{-/-}$). To gain further insights into the critical physiological functions of *Npy6r* in mice, we also used our $Npy6r^{-/-}$ mouse model to determine the physiological ligand for this Y-receptor in vivo.

RESULTS

$Npy6r^{-/-}$ Mice Are Viable and Have Normal Fertility

Npy6r gene deletion was achieved by inserting a *lacZ*-IRES-*neoR* selection cassette into the coding frame of the *Npy6r* gene, allowing for identification of normal sites of gene expression via X-gal staining for β-galactosidase (Figure 1A). $Npy6r^{-/-}$ mice were identified by PCR (Figure 1B) and confirmed by RT-PCR in various tissues (Figure 1C). Utilizing the introduced *lacZ* gene, we investigated the expression pattern of *Npy6r* in a variety of peripheral tissues and throughout the brain (see Figures S1 and S2 online). Only a subset of neurons within the hypothalamic supracharismatic nucleus (SCN) showed staining for β-gal, with no staining in any other area of the brain or the peripheral tissues examined, except testes. This demonstrates that *Npy6r* signaling in the brain is restricted to the SCN.

$Npy6r^{-/-}$ mice are viable; however, they are smaller than their wild-type (WT) counterparts (Figure 1D). Breeding of heterozygous $Npy6r^{+/-}$ mice resulted in live offspring with a genotype frequency not different from the expected Mendelian ratio (Table S1). Since *Npy6r* are expressed in the testes, we investigated whether deletion of this receptor impacts on fertility. Homozygous $Npy6r^{-/-}$ breeding pairs produced litters of a similar size to litters from WT and heterozygous breeding pairs (Table S1). Additionally, the mortality rate and gender ratio of pups born from heterozygous and homozygous breeding pairs did not significantly differ from that of WT (Table S1), further suggesting that disruption of *Npy6r* expression does not have any impact upon reproductive fitness.

Lack of *Npy6r* Signaling Leads to an Early Reduction in Body Weight, Reduced Lean Mass, and the Development of Late-Onset Obesity

$Npy6r^{-/-}$ mice showed reduced body weights relative to WT mice from 6 to 23 weeks of age but were no longer different at 24 weeks of age (Figure 1E). $Npy6r^{-/-}$ mice showed markedly reduced lean body mass when analyzed by whole-body dual-energy X-ray absorptiometry (DXA) at 9, 15, 20, and 24 weeks of age (Figure 1F). Importantly, lean body mass as a percent of body weight was also lower in 20- and 24-week-old $Npy6r^{-/-}$ mice compared to WT mice (Figure 1G), suggesting a disproportionate reduction in lean mass in the knockouts. Deletion of *Npy6r* also led to a transient reduction in absolute fat mass at 15 weeks of age (Figure 1F), but at 20 or 24 weeks of age, $Npy6r^{-/-}$ mice showed greater adiposity (Figures 1F and IG). Consistent with the DXA scan results, the absolute or relative weights of dissected white adipose tissues depots from the inguinal (i), epididymal (e), retroperitoneal (r), and mesenteric (m) sites and the brown adipose tissue (b) were significantly reduced in the absence of *Npy6r* in 15-week-old mice (Figures 1H and 1I). In contrast to this reduction in adiposity at an early age, the weights of dissected white and brown adipose tissue depots were markedly greater in 24-week-old $Npy6r^{-/-}$ mice (Figures 1J and 1K).

Since obesity is associated with ectopic lipid deposition in various tissues including the liver, we investigated this in our $Npy6r^{-/-}$ mice. Interestingly, we found a significant increase in liver weight relative to body weight in $Npy6r^{-/-}$ mice at 15 weeks of age (Figure 1L). This was associated with a significantly greater amount of lipid in the livers of these mice (Figure 1M), as determined by oil red O staining (Figure 1O). Consistent with this, 24-week-old $Npy6r^{-/-}$ mice also exhibited significantly higher hepatic lipid accumulation (Figures 1N and 1P). Since $Npy6r^{-/-}$ mice showed reduced adiposity at 15 weeks of age (Figures 1F, 1H, and 1I), this result suggests that ectopic fat accumulation in the liver precedes the development of age-induced fat accumulation in $Npy6r^{-/-}$ mice.

Reduced Body Weight and Preferential Fat Accumulation in $Npy6r^{-/-}$ Mice Are Associated with Increased Cumulative Food Intake Relative to Body Weight

To determine if the reduction in body weight and altered body composition in $Npy6r^{-/-}$ mice could be explained by changes in feeding behavior, we analyzed the food intake of $Npy6r^{-/-}$ and WT mice. Spontaneous food intake and spillage did not differ significantly between genotypes at 15 weeks of age (Figure 2A). However, $Npy6r^{-/-}$ mice exhibited a trend toward increased daily food intake at 24 weeks of age (Figure 2B). In spite of this, $Npy6r^{-/-}$ mice displayed significantly greater fecal output at 15, but not at 24, weeks of age (Figures S3A and S3B). Following a 24 hr fast at 13 weeks of age, food intake, spillage (Figure 2C), and fecal output (Figure S3C) were similar between $Npy6r^{-/-}$ and WT mice. Since food spillage was not significantly different between $Npy6r^{-/-}$ and WT mice, we also monitored food intake as the amount of food removed from the hopper over the entire period between 16 and 22 weeks of age and found no significant difference in cumulative food consumption (Figure 2D). Importantly, however, these differences were statistically significant when normalized for body weight (Figure 2E), indicating that increased food intake may contribute to the increased adiposity and weight gain in older $Npy6r^{-/-}$ mice.

Indirect calorimetry on 14-week-old $Npy6r^{-/-}$ mice revealed a significant increase in energy expenditure compared to WT, either when expressed as absolute values (Figure 2F) or when

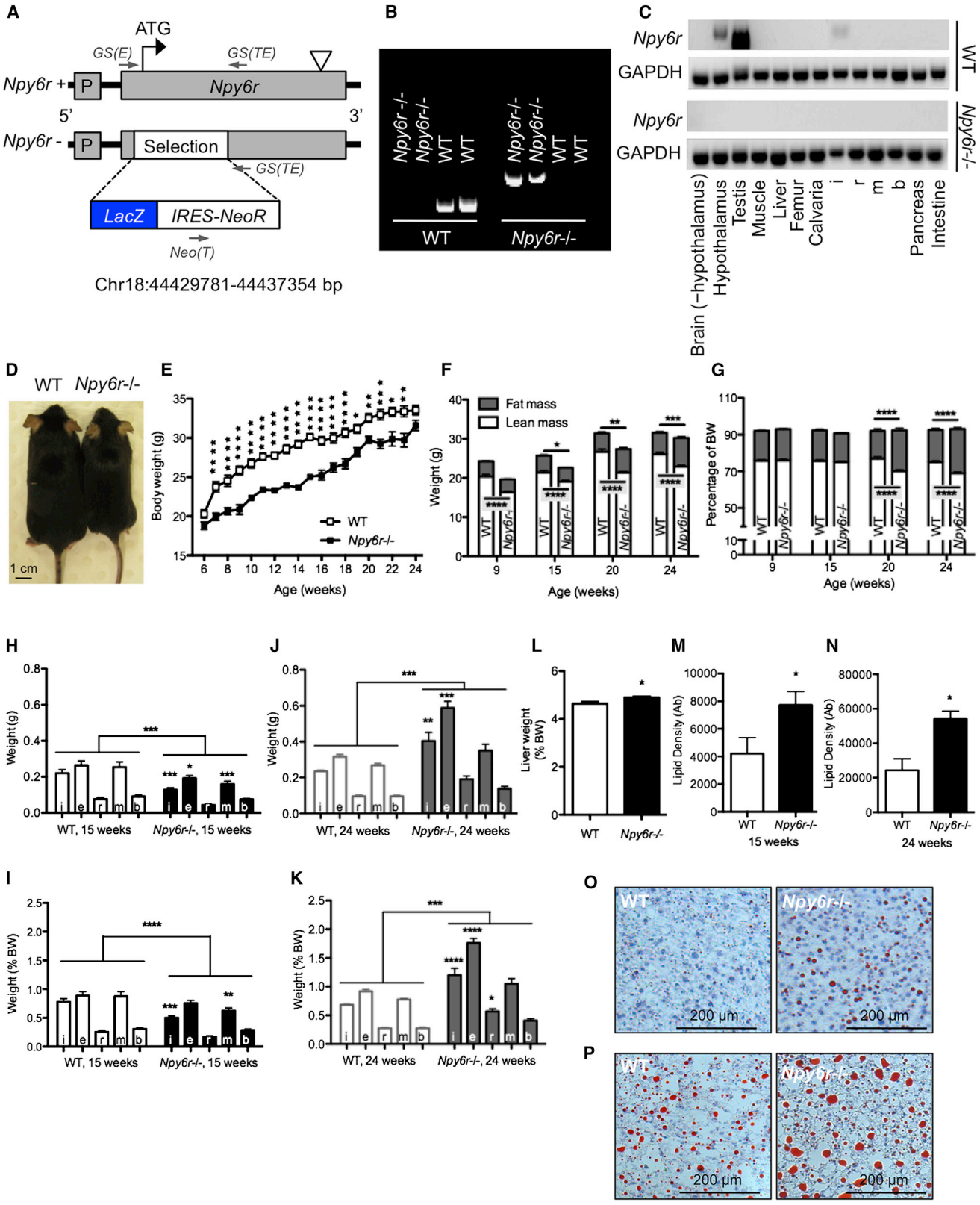

Figure 1. Chow-Fed *Npy6r*$^{-/-}$ Mice Exhibit Reduced Body Weight, Lean Mass, and Late-Onset Obesity

(A) Generation of the *Npy6r*-deficient mice.

(B) Genotyping was performed using GS(E)/GS(TE) or Neo(T)/GS(TE) primer pairs to amplify WT or knockout (*Npy6r*$^{-/-}$) alleles, respectively.

(legend continued on next page)

normalized for lean body mass (Figure 2G). Associated with this, *Npy6r*$^{-/-}$ mice exhibited significantly increased activity (Figure 2H). We further inquired if changes in resting metabolic rate could also contribute to the observed increase in energy expenditure in *Npy6r*$^{-/-}$ mice by analyzing the energy expenditure corresponding to the hour of least activity and found no significant difference (Figures S4A and S4B; Table S2). In addition, we assessed resting metabolic rate by extrapolating regression lines of energy expenditure to physical activity (Zhang et al., 2010) and found that resting energy expenditure is not significantly different between 14-week-old *Npy6r*$^{-/-}$ and WT mice (Figures S4A and S4B; Table S2). These results indicate that the absence of *Npy6r* signaling does not increase basal metabolic rate, and that the increase in energy expenditure observed in 14-week-old *Npy6r*$^{-/-}$ mice was most likely due to the increase in physical activity.

In addition to increased energy expenditure, 14-week-old *Npy6r*$^{-/-}$ mice demonstrated a significant elevation in respiratory exchange ratio (RER), indicative of a reduction in lipid utilization for whole-body energy production (Figure 2I). While the elevated RER in *Npy6r*$^{-/-}$ mice may reflect the reduced adiposity in 15-week-old *Npy6r*$^{-/-}$ mice (Figures 1F and 1H), an RER value greater than 1.0, as seen in *Npy6r*$^{-/-}$ mice between 22:00 and 02:00 hr (Figure 2I), is associated with de novo lipogenesis (Schutz, 2004). Since an increase in RER has been demonstrated to predict weight gain (Marra et al., 2004; Seidell et al., 1992; Weinsier et al., 1995), these data are in line with the development of a late-onset increase in adiposity in *Npy6r*$^{-/-}$ mice.

Secondary to the age-induced increase in adiposity, 23-week-old *Npy6r*$^{-/-}$ mice displayed a significant reduction in RER (Figure 2J), suggesting an increased preference for lipids as an oxidative fuel source. Consistent with the increased energy expenditure and physical activity seen in 14-week-old *Npy6r*$^{-/-}$ mice, 23-week-old *Npy6r*$^{-/-}$ showed significant increases in energy expenditure when normalized for lean mass (Figures 2K and 2L), as well as an increase in physical activity during the light phase (Figure 2M). Furthermore, resting energy expenditure was significantly higher in *Npy6r*$^{-/-}$ mice at 23 weeks of age (Figures S4C and S4D; Table S2). These data suggest that, in addition to increased physical activity, an increase in basal metabolic rate is an important contributor to the increased total energy expenditure observed in 23-week-old *Npy6r*$^{-/-}$ mice.

Npy6r Signaling Is Critical for Maintaining Glucose Homeostasis in Mice

Skeletal muscle is a major site of insulin-mediated glucose disposal, and a reduction in lean mass is associated with impairment in glucose homeostasis and insulin sensitivity (Dulloo, 2009). Since *Npy6r*$^{-/-}$ mice demonstrated a significant reduction in lean body mass, we suspected that glucose metabolism might be impaired in these mice. Interestingly, 15-week-old *Npy6r*$^{-/-}$ mice exhibited normoglycemia under fasted and nonfasted conditions (Figure 3A). Despite this, *Npy6r*$^{-/-}$ mice at 15 weeks of age exhibited reduced serum insulin concentrations, significantly so in the nonfasted condition (Figure 3B), suggesting improved insulin action on glucose clearance. Indeed, in response to i.p. glucose administration, the area under the curve for the glucose tolerance tests were significantly reduced in 15-week-old *Npy6r*$^{-/-}$ mice (Figures 3C and 3D) despite significantly lower serum insulin concentrations (Figure 3E).

In contrast, while fasted and nonfasted blood glucose levels were similar between 24-week-old *Npy6r*$^{-/-}$ and WT mice (Figure 3F), the heightened fat accumulation in *Npy6r*$^{-/-}$ mice of this age is accompanied by a significant elevation in nonfasting serum insulin concentrations (Figure 3G), suggesting decreased insulin action in older *Npy6r*$^{-/-}$ mice. Consistent with this, we found that insulin signaling in muscle and liver, as determined by Akt phosphorylation, is reduced in 24-week-old *Npy6r*$^{-/-}$ mice (Figures S5A and S5B). Despite this, *Npy6r* deficiency did not result in deterioration in glucose tolerance, with blood glucose and serum insulin levels in response to i.p. glucose injection being similar between 24-week-old *Npy6r*$^{-/-}$ and WT mice (Figures 3H and 3I).

Npy6r$^{-/-}$ Mice Show Exacerbated Diet-Induced Obesity

We next assessed the effect of *Npy6r* deletion in mice on a high-fat diet (HFD), which was introduced at 7 weeks of age and continued for 16 weeks. Relative to WT, *Npy6r*$^{-/-}$ mice exhibited significantly lower starting body weights (Figure 4A) but displayed significantly greater relative body weight gain on the HFD (Figure 4B). Importantly, after 8 weeks on the HFD (i.e., 15 weeks of age) *Npy6r*$^{-/-}$ mice showed similar body weights to age-matched WT controls (Figure 4A), showing that the normalization of body weight in 24-week-old chow-fed *Npy6r*$^{-/-}$ mice seen in Figure 1E was accelerated by the obesogenic diet.

Consistent with the effect of *Npy6r* deletion in mice on a normal chow diet (Figures 1F and 1G), HFD-fed *Npy6r*$^{-/-}$ mice displayed reduced lean body mass as determined by whole-body DXA scans and when expressed as either absolute weight or as a percent of body weight (Figures 4C and 4D). *Npy6r*$^{-/-}$ mice also showed significantly higher adiposity at 7 and 14 weeks after the commencement of HFD feeding (Figures 4C and 4D). This greater adiposity was confirmed by significantly greater absolute and relative masses of dissected white and brown adipose tissue depots in *Npy6r*$^{-/-}$ mice after 16 weeks on the HFD (Figures 4E and 4F). These data show that, together with the suppression of lean body mass, the impact of *Npy6r*

(C) *Npy6r* mRNA expression was determined in various tissues, including the hypothalamus, testes, and inguinal white adipose tissue (i), by RT-PCR using GAPDH as a housekeeping gene.
(D) A representative photograph of 15-week-old WT and *Npy6r*$^{-/-}$ mice.
(E) Body weight in *Npy6r*$^{-/-}$ and WT mice was measured on a weekly basis.
(F and G) Body composition (lean and fat mass) was determined by DXA and normalized to body weight at indicated time points in *Npy6r*$^{-/-}$ and WT mice.
(H–K) Absolute and relative (as a percent of body weight) weights of white adipose tissues from the inguinal (i), epididymal (e), mesenteric (m), and retroperitoneal (r) sites, and intrascapular brown adipose tissue (b) depots were measured in 15- and 24-week-old *Npy6r*$^{-/-}$ and WT mice.
(L–N) (L) Liver weight and (M and N) liver morphology were determined by the quantity of oil red O staining from 15- and 24-week-old *Npy6r*$^{-/-}$ and WT mice.
(O and P) Representative oil red O-stained liver sections from WT and *Npy6r*$^{-/-}$ mice. Data are means ±SEM of 5–13 mice per group. See also Figures S1 and S2 and Table S1.

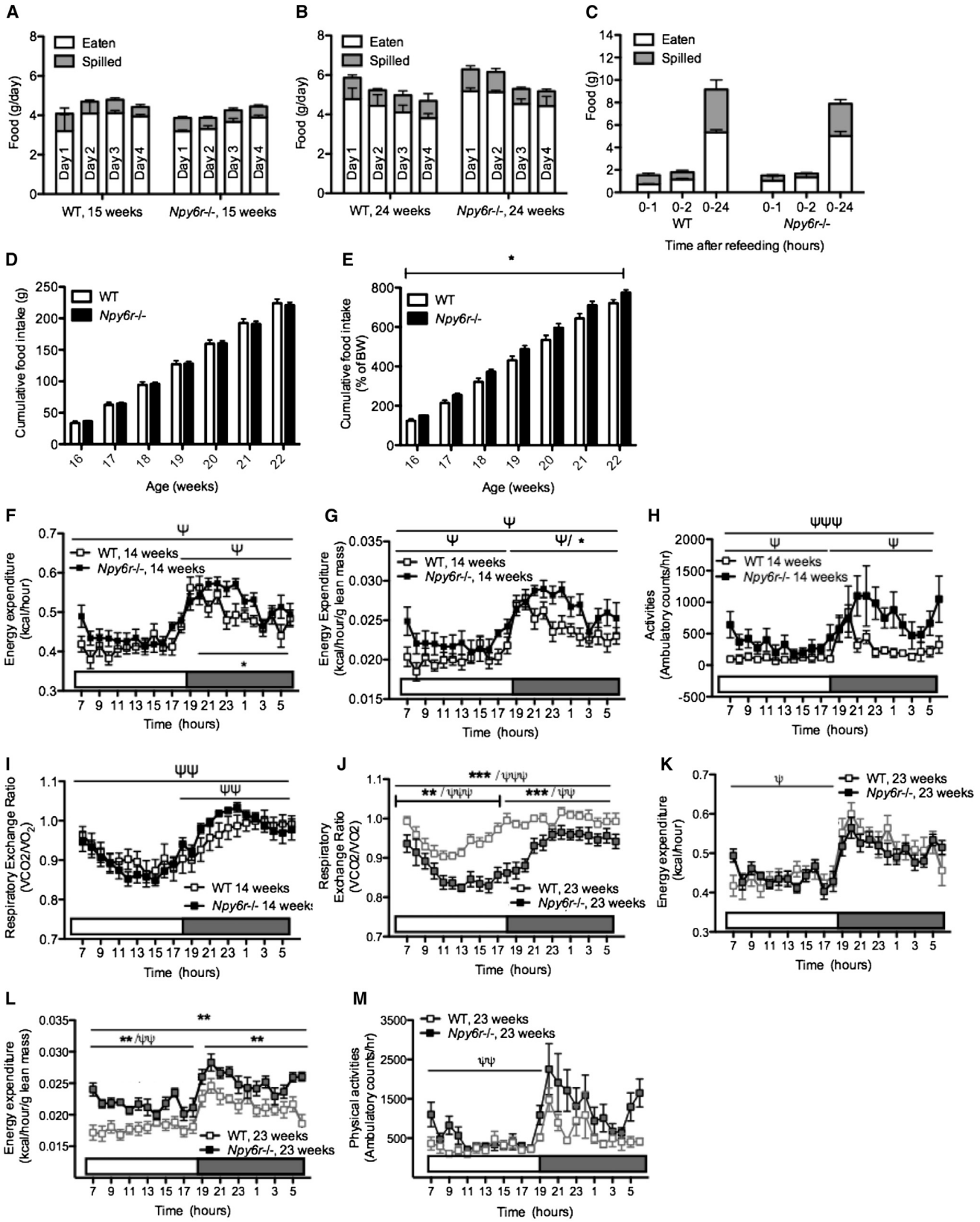

(legend on next page)

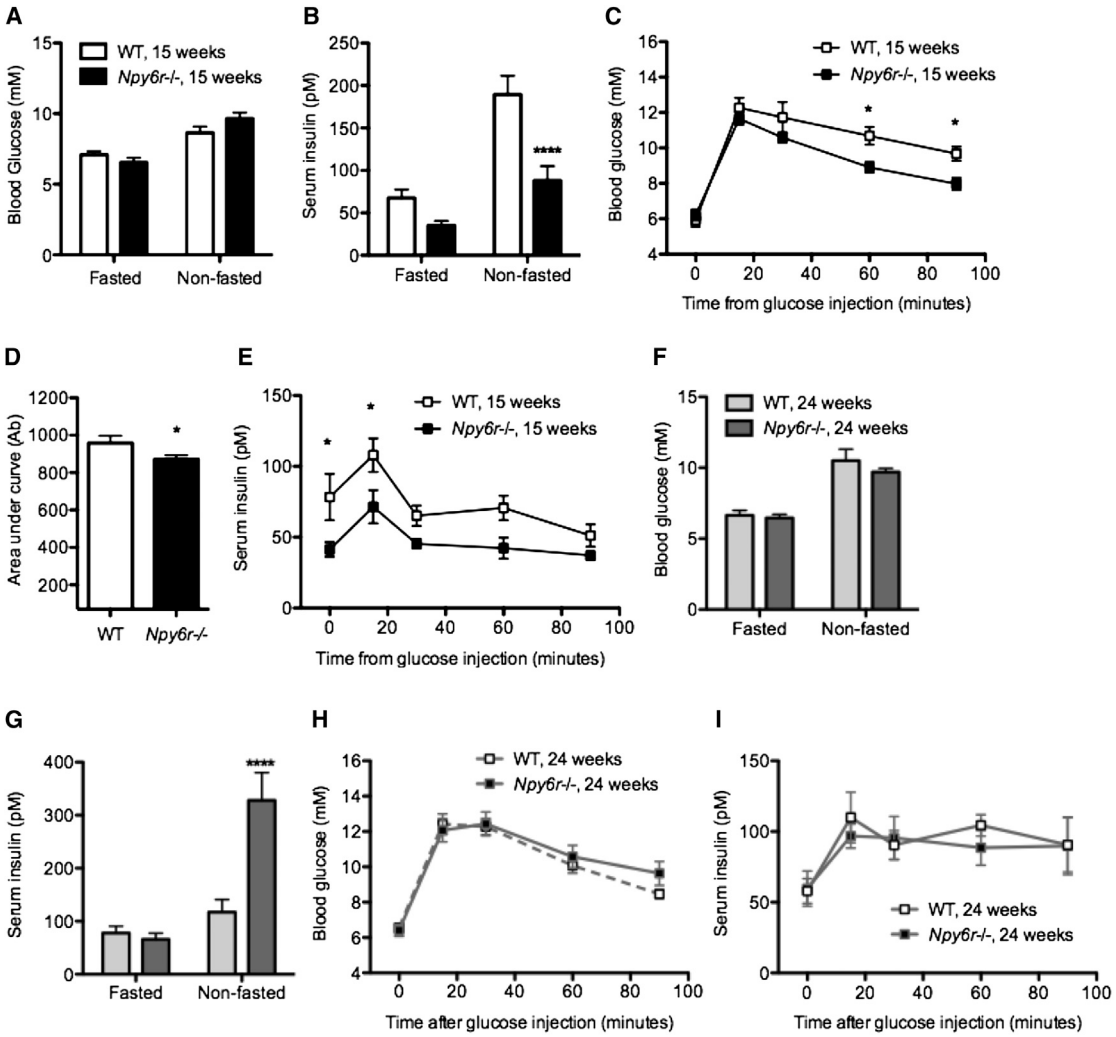

Figure 3. Impact of *Npy6r* Deletion on Glucose Homeostasis in Mice

(A and B) Fasted and nonfasted blood glucose and serum insulin levels in 15- and (F and G) 24-week-old *Npy6r*$^{-/-}$ and WT mice were determined. (C–E) Fifteen- and (H and I) 24-week-old *Npy6r*$^{-/-}$ and WT mice were fasted, and glucose tolerance tests (1 mg/kg) were performed. Blood glucose and corresponding serum insulin levels were assessed at indicated time points in these mice. Results are means ±SEM of 5–11 mice per group. See also Figure S5.

deficiency in enhancing adiposity in mice is exacerbated by the HFD.

Interestingly, the exacerbated body weight gain and adipose tissue accumulation in *Npy6r*$^{-/-}$ mice on a HFD occurred in the presence of transient hyperphagia. While food intake in absolute weight did not differ significantly between genotypes at 3 weeks after the introduction of HFD (Figure 4G), *Npy6r*$^{-/-}$ mice consumed significantly more HFD relative to their body weights compared to WT controls at this time point (Figure 4H). In contrast, food intake of *Npy6r*$^{-/-}$ mice was significantly reduced after 13 weeks on the HFD (Figures 4G and 4H). Reflective of the changes in absolute food consumption (Figure 4G), fecal output was significantly reduced after 10 but not 3 weeks of high-fat feeding in *Npy6r*$^{-/-}$ mice (Figure S3D). In response to a 24 hr fast, young *Npy6r*$^{-/-}$ mice exhibited no change in food intake (Figures 4I and 4J) or fecal output (Figure S3E), whereas older knockouts demonstrated a significant reduction in fasting-induced food intake (Figures 4K and 4L) and fecal output (Figure S3F). The transient increase in nonfasted food intake relative to body weight seen at 3 weeks after the provision of HFD (Figure 4H) may contribute to the accelerated body weight gain in HFD-fed *Npy6r*$^{-/-}$ mice. Additionally, since

Figure 2. Altered Food Intake and Energy Homeostasis in *Npy6r*-Deficient Mice

(A–C) Daily and 24 hr fasting-induced food intake and spillage were assessed in *Npy6r*$^{-/-}$ and WT mice at indicated time points.

(D and E) Cumulative food consumption from 16- to 22-week-old *Npy6r*$^{-/-}$ and WT mice were recorded and normalized to total body weight.

(F–M) Light and dark cycle energy expenditure (normalized to total lean mass), ambulatory activity, and respiratory exchange ratio (RER) were determined in metabolic chambers during indirect calorimetry studies in 14- and 23-week-old *Npy6r*$^{-/-}$ and WT mice. Significant time and genotype interaction effects are indicated by Ψ. Data are means ±SEM of five to nine mice per group. See also Figures S3 and S4 and Table S2.

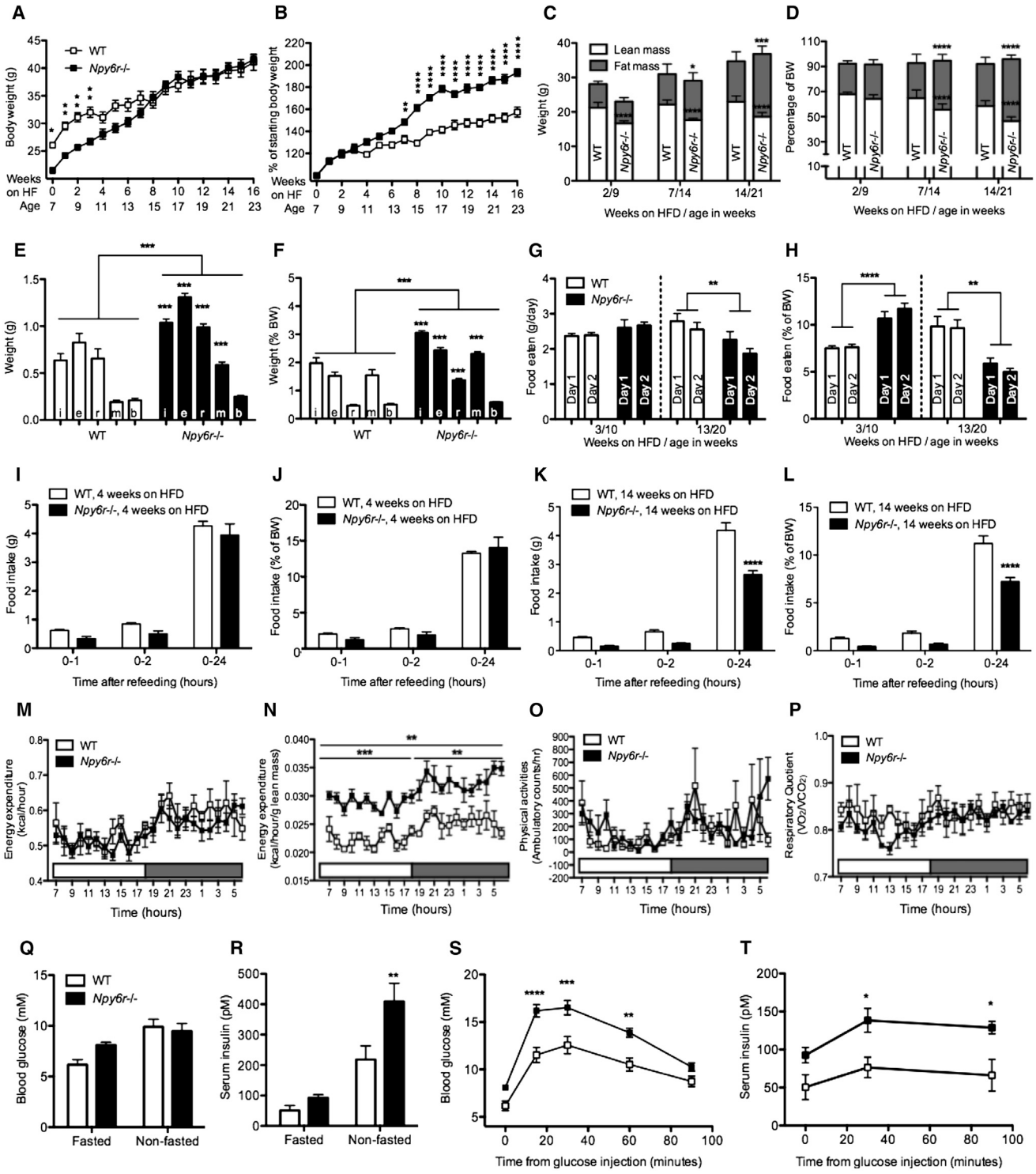

Figure 4. Mice Lacking *Npy6r* Showed Exacerbated Diet-Induced Obesity

(A and B) Seven-week-old *Npy6r*$^{-/-}$ and WT mice underwent high-fat feeding for 16 weeks, and body weight was monitored on a weekly basis.

(C and D) Body composition (lean and fat mass) was determined by DXA and subsequently normalized to body weight.

(E and F) Weight of white adipose tissues from the inguinal (i), epididymal (e), mesenteric (m), and retroperitoneal (r) sites, and intrascapular brown adipose tissue (b) depots in high-fat-fed *Npy6r*$^{-/-}$ and WT mice were measured and expressed as absolute weight or as a percentage of body weight.

(G and H) Daily food intake in high-fat-fed *Npy6r*$^{-/-}$ and WT mice was recorded.

(I–L) Mice were fasted for 24 hr, and fasting-induced food intake was determined at indicated time points. Food intake results were expressed in absolute terms or as a percentage of body weight.

(legend continued on next page)

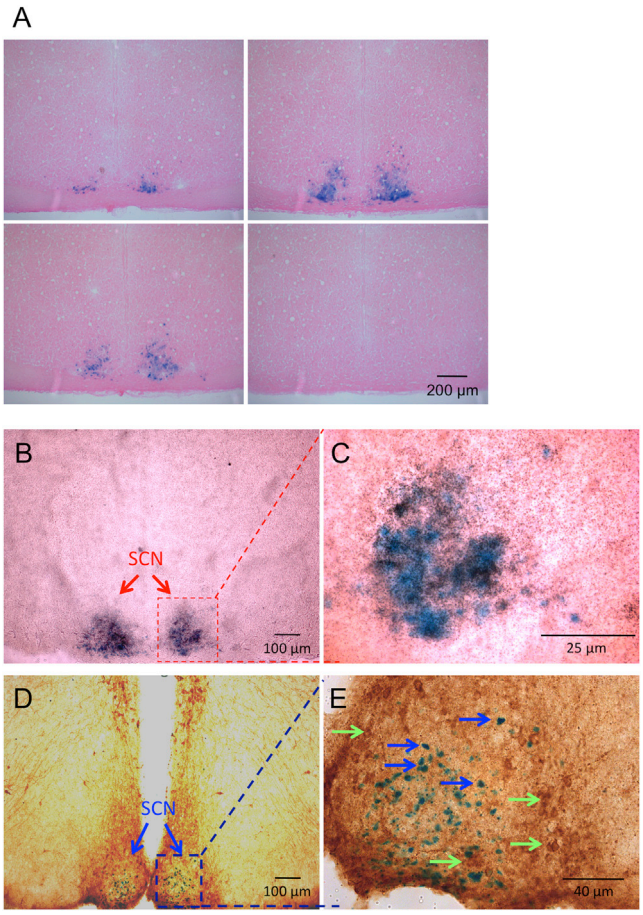

Figure 5. *Npy6r* Deficiency Is Associated with Reduced *Vip* Expression in the SCN

(A) Representative photographs of coronal brains sections showing the distribution of *Npy6r* as indicated by *lacZ* expression in the mouse SCN.

(B and C) Representative photographs showing coexpression of *lacZ* and *Vip* mRNA in neurons of the SCN of *Npy6r*$^{-/-}$ mice.

(D and E) Representative photographs showing the absence of *lacZ* and arginine vasopressin (AVP) colocalization in the suprachiasmatic nucleus (SCN) of *Npy6r*$^{-/-}$ mice. Light green and dark blue arrows denote neurons expressing only AVP and only *lacZ*, respectively. See also Figure S6.

nonfasted and fasting-induced food intake at the later time point were significantly reduced, lack of *Npy6r* in mice may lead to increased feeding efficacy and greater body weight gain seen in HFD-fed *Npy6r*$^{-/-}$ mice.

Using indirect calorimetry we identified that after 14 weeks on the HFD, *Npy6r*$^{-/-}$ mice did not exhibit any difference in absolute energy expenditure (Figure 4M). When adjusted for the difference in lean body mass, however, energy expenditure was significantly greater in HFD-fed *Npy6r*$^{-/-}$ mice (Figure 4N). This increase in energy expenditure was more pronounced than that seen in chow-fed *Npy6r*$^{-/-}$ mice at either the younger age or the older age (Figures 2G and 2L). Unlike in chow-fed animals (Figure 2H–2J and 2M), we did not detect any significant differences in physical activity (Figure 4O) or RER (Figure 4P) between HFD-fed *Npy6r*$^{-/-}$ and WT mice. These results show that the increase in body weight gain and fat accumulation in *Npy6r*$^{-/-}$ mice on the HFD is not due to reduced metabolism.

Interestingly, after 12 weeks on the HFD, *Npy6r*$^{-/-}$ mice still displayed normoglycemia (Figure 4Q) but showed elevated serum insulin levels, significantly so in the nonfasted state (Figure 4R). However, when assessed for glucose tolerance, *Npy6r*$^{-/-}$ mice on HFD displayed markedly higher blood glucose (Figure 4S) and serum insulin levels (Figure 4T) in response to i.p. glucose injection, signifying impaired glucose metabolism. Taken together, our data demonstrate that deficiency in *Npy6r* in mice exacerbates diet-induced obesity and promotes the associated abnormalities in glucose homeostasis.

Npy6r$^{-/-}$ Mice Have Impaired Central VIP Signaling in Association with Reduced Serum IGF-1 and Blunted Corticosterone Rhythm

In order to identify the underlying mechanism that leads to the altered metabolic phenotype of *Npy6r* deficiency, we focused on areas of highest *Npy6r* expression. As shown in Figures 5A, S1, and S2, the strongest expression of *Npy6r* was found in the hypothalamic SCN, with expression also detected in the testes. It is known that reduction in circulating testosterone levels is strongly linked to reduced lean body mass (Sattler et al., 2009) and obesity (Nettleship et al., 2007). However, *Npy6r*$^{-/-}$ mice did not show reduced serum testosterone levels (Figure S6A), suggesting that this is not a major contributor to the observed phenotype.

In order to elucidate possible pathways by which *Npy6r* signaling may regulate energy balance and body composition, we determined the molecular identity of *Npy6r*-expressing neurons in the SCN by utilizing the introduced *lacZ* gene into the *Npy6r* gene coding region to visualize the expression pattern of *Npy6r* by staining for β-gal. Immunostaining with antibodies against a variety of neuropeptides known to be expressed in the SCN (Reghunandanan et al., 1993) revealed vasoactive intestinal peptide (VIP) as colocalized with the *Npy6r* (Figures S6B and S6C). To further confirm this colocalization, we performed in situ hybridization for *Vip* mRNA on SCN sections previously stained for *LacZ*. As shown in Figures 5B and 5C, almost all *LacZ*-positive neurons express VIP, shown in the overlaying silver grains. In contrast, immunostaining using arginine vasopressin (AVP) antibody did not show any overlap in expression with *Npy6r*-positive neurons (Figures 5D and 5E).

PP Is the Endogenous High-Affinity Ligand for the *Npy6r* in Mice

The SCN receives input from a variety of areas in the brain (Welsh et al., 2010). Additionally, the SCN is accessible to factors derived from the circulation (Welsh et al., 2010), including peripherally derived PP and PYY. To investigate which Y-receptor ligand is the most effective transducer of *Npy6r* function in vivo,

(M–P) After 12 weeks of high-fat feeding, energy expenditure, ambulatory activity, and respiratory exchange ratio (RER) were determined.

(Q and R) Fasted and nonfasted blood glucose and serum insulin levels were determined.

(S and T) Mice were fasted for 6 hr and injected with glucose (1 mg/kg). Blood glucose and corresponding insulin levels at indicated time points were assessed. Data are means ±SEM of nine males per group. See also Figure S3.

we examined the expression of Fos in the SCN of *Npy6r*$^{-/-}$ and WT mice in response to i.p. administration of either PP, PYY, PYY3-36, or saline. Injection of PYY or PYY3-36 into WT mice did not induce any significant differences in Fos expression in the SCN compared to saline controls (Figure 6A) but significantly increased Fos expression in other areas like the arcuate nucleus (ARC) (data not shown). Importantly, a significant increase in Fos immunoreactivity in the SCN of WT mice was seen following i.p. PP injection, and this effect was absent in *Npy6r*$^{-/-}$ mice (Figures 6A and 6B). To further confirm this, we performed radioligand-binding assays on brain sections from WT and *Npy6r*$^{-/-}$ mice using I^{125}-labeled PP. Supporting the notion that PP is a physiological activator of *Npy6r*, I^{125}-labeled PP binding was detected in the SCN of WT mice, but not in *Npy6r*$^{-/-}$ brain sections (Figure S7A). By contrast, the binding of I^{125}-labeled PP was not observed in WT brain slices cotreated with human PP (Figure S7A). This raises the possibility that increases in circulating PP levels due to food intake or hypoglycemia can trigger *Npy6r*-mediated events in the SCN.

Previous studies have shown that extracellular signal-related kinase (ERK) is involved in mediating downstream signaling of Y receptors, including the *Npy1r* (Shi et al., 2013). To investigate whether ERK may also act as a downstream substrate for the *Npy6r* in response to PP, we injected WT and *Npy6r*$^{-/-}$ mice with either saline or PP and assessed ERK phosphorylation (p-ERK) by immunohistochemistry. While PP-induced p-ERK in the SCN region was elevated in WT mice compared to saline-injected controls, induction of pERK was strongly reduced in the SCN of *Npy6r*$^{-/-}$ mice in response to PP (Figure 6C). Taken together, these results are in keeping with the notion that PP is a physiological ligand for *Npy6r* and that ERK is an important downstream substrate for *Npy6r* signaling.

Strong evidence exists that PP regulates energy homeostasis by decreasing food intake and increasing energy expenditure via action on *Ppyr1* (Lin et al., 2009). Our findings that PP also activates the *Npy6r* raised the possibility that PP could regulate energy balance and appetite separately via an *Npy6r* signaling pathway. To examine this directly, both WT and *Npy6r*$^{-/-}$ mice were given an i.p. injection of saline or PP at 7 a.m. and 7 p.m., with subsequent monitoring of oxygen consumption, energy expenditure, and fasting-induced food intake. Consistent with previous studies, we found that oxygen consumption and energy expenditure were significantly increased in WT mice in response to PP injection (Figures 6D and 6E). However, these differences were not noted in *Npy6r*$^{-/-}$ mice (Figures 6D and 6E), indicating that *Npy6r* is required to mediate the effects of PP in the regulation of energy expenditure. In response to PP, both WT and *Npy6r*$^{-/-}$ mice exhibited reductions in fasting-induced food intake compared to the corresponding saline group, significantly so in WT animals (Figures 6F and 6G). However, the degree to which PP suppressed food intake was significantly less in *Npy6r*$^{-/-}$ mice at an early time point (0–4 hr), and these differences were even greater when normalized for body weight (Figures 6F and 6G).

PP-Mediated *Npy6r* Signaling Controls *Vip* Expression in the SCN

Having established that *Npy6r* are coexpressed with VIP in neurons of the SCN, we hypothesized that the metabolic phenotype of *Npy6r*$^{-/-}$ mice may be explained by impairment in downstream actions of VIP. We determined *Vip* mRNA levels in the hypothalamus of WT and *Npy6r*$^{-/-}$ mice by quantitative real-time PCR. Consistent with our hypothesis of impaired VIP signaling, we found that *Vip* expression was significantly reduced in the hypothalamus of *Npy6r*$^{-/-}$ (Figure 7A), but not in other peripheral tissues such as colon, small intestine, or pancreas (Figure S7B). Lack of change in peripheral *Vip* mRNA levels is consistent with unaltered serum VIP levels in *Npy6r*$^{-/-}$ mice (Figure S7C). Additionally, *Vip* expression levels in the SCN of *Npy6r*$^{-/-}$ were significantly reduced as determined by in situ hybridization (Figures 7B and 7C), confirming that VIP signaling is disrupted in the SCN of *Npy6r*$^{-/-}$ mice.

VIP is known as a key regulator of the growth hormone (GH) axis (Asnicar et al., 2002; Niewiadomski et al., 2008), circadian rhythm (Aton et al., 2005; Brown et al., 2007; Pantazopoulos et al., 2010; Piggins and Cutler, 2003), and glucocorticoid secretion (Loh et al., 2008). Previous studies showed that VIP-deficient mice exhibit reduced IGF-1 levels (Asnicar et al., 2002; Niewiadomski et al., 2008), and perturbation in the GH/IGF-1 axis is associated with dwarfism and increased adiposity in rodents and humans (Lichanska and Waters, 2008). We thus hypothesized that the GH/IGF-1 axis is perturbed in *Npy6r*$^{-/-}$ mice and that this contributes to the development of reduced lean mass and late-onset obesity. Indeed, *Npy6r*$^{-/-}$ mice showed significantly reduced serum IGF-1 levels (Figure 7D), coinciding with a reduction in hypothalamic expression of growth hormone releasing hormone (*Ghrh*) (Figure 7E). Additionally, loss of *Npy6r* in mice led to blunted diurnal variations in serum corticosterone levels (Figure 7F). Importantly, the damped corticosterone rhythm seen in *Npy6r*$^{-/-}$ mice is not due to impaired secretion, since a 24 hr fast elicited comparable increases in corticosterone levels in mice of both genotypes, although *Npy6r*$^{-/-}$ mice showed significantly reduced corticosterone levels compared to WT controls under both fed and fasted conditions (Figure 7G). Since timing of food intake is linked to corticosterone secretion (Sheward et al., 2007) and has been shown to be abrogated in mice with disrupted VIP signaling (Bechtold et al., 2008), we investigated food consumption during light and dark phases and found significantly reduced daytime feeding in *Npy6r*$^{-/-}$ mice (Figures 7H and 7I). Hence, our data provide evidence that the reduced lean mass and late-onset or diet-induced increases in adiposity in mice lacking *Npy6r* may result from reduced hypothalamic *Ghrh* expression and circulating IGF-1 levels, potentially attributable to impairment in VIP signaling in the SCN.

Further evidence supporting the notion of a PP-controlled GH/IGF-1 axis comes from experiments in which we injected PP via the i.c.v. route and measured the consequences on *Ghrh* mRNA expression in WT compared to *Npy6r*$^{-/-}$ mice. While i.c.v. administration of PP to WT mice led to a significant increase in *Ghrh* mRNA levels in the ARC, this PP-dependent effect was absent in *Npy6r*$^{-/-}$ mice (Figures 7J and 7K). Together with our findings of SCN-specific *Npy6r* expression, colocalization of *Npy6r* with VIP in the SCN, reduced expression of *Vip* mRNA in the SCN of *Npy6r*$^{-/-}$ mice, and PP-induced Fos activation in the SCN, these data indicate that alterations in GH/IGF-1 axis activity in *Npy6r*$^{-/-}$ mice are a direct consequence of the lack of PP-induced activation of *Npy6r* in the SCN, possibly via VIP.

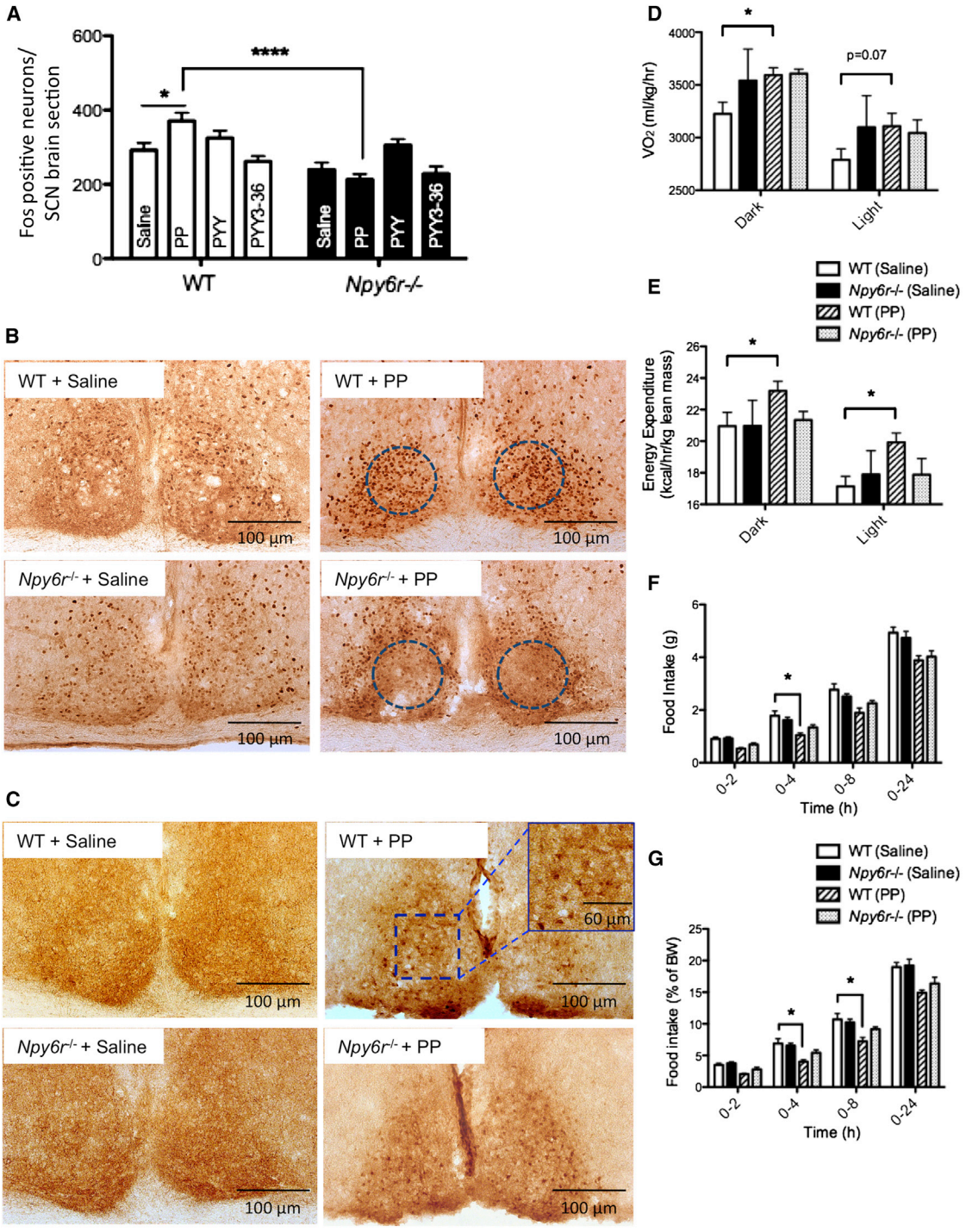

Figure 6. Pancreatic Polypeptide Is the Endogenous Ligand for the *Npy6r* In Vivo

(A and B) WT and *Npy6r*$^{-/-}$ mice were injected with either saline, PP (200 µg/kg), PYY (200 µg/kg), or PYY 3-36 (200 µg/kg). Fos expression in the suprachiasmatic nucleus (SCN) of the hypothalamus was assessed by immunohistochemistry after 30 min injection. Fos-positive neurons in SCN brain sections were quantified.

(C) WT and *Npy6r*$^{-/-}$ mice were injected with either saline or PP, and PFA perfused brains were extracted and processed for immunohistochemistry with antibodies to p-ERK.

(D and E) WT and *Npy6r*$^{-/-}$ mice were injected with either saline or PP (300 µg/kg) as indicated, and oxygen consumption and energy expenditure were monitored by indirect calorimetry.

(F and G) WT and *Npy6r*$^{-/-}$ mice were fasted for 24 hr, and prior to food being given mice were injected with either saline or PP (300 µg/kg) as indicated. Fasting-induced food intake was determined for a period of 24 hr. Data are means ±SEM of three to six mice per group. See also Figure S7.

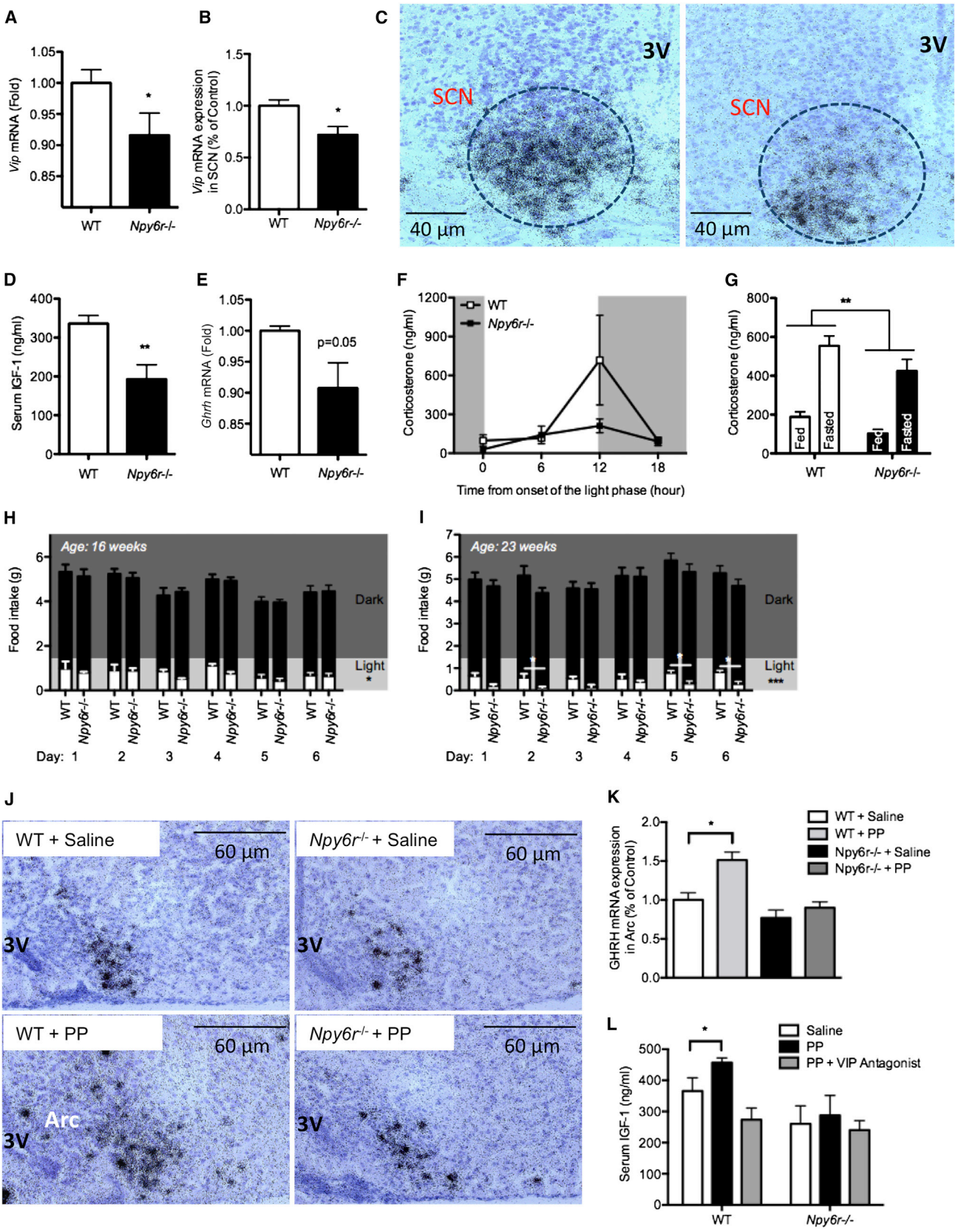

(legend on next page)

Finally, to demonstrate that alterations in downstream VIP signaling are linked to the observed changes in energy homeostasis such as the reduction of IGF-1 levels, we delivered VIP(6-28), a VPAC receptors antagonist, via the i.c.v. route to WT and *Npy6r*$^{-/-}$ mice, followed 5 min later by i.p. administration of PP. Analysis of serum samples collected 30 min following PP injection revealed that blockade of VPAC receptors in WT mice completely prevented the PP-induced increase in serum IGF-1 in WT mice (Figure 7L). Furthermore, the effect of PP to raise serum IGF-1 was totally absent in *Npy6r*$^{-/-}$ mice (Figure 7L), clearly demonstrating involvement of *Npy6r* signaling via VIP in controlling the growth hormone axis.

DISCUSSION

In this study, we demonstrate that *Npy6r* signaling in the SCN is critical in the regulation of energy homeostasis. Our results show that body weight, body composition, metabolic rate, and activity of the hypothalamo-pituitary-somatotrophic axis are significantly influenced by *Npy6r* signaling in mice, since lack of *Npy6r* leads to reduced lean mass and increased energy expenditure that are accompanied by significant improvements in glucose homeostasis and reduced hypothalamic *Ghrh* mRNA expression and circulating IGF-1 levels. Interestingly, *Npy6r*-deficient mice develop late-onset obesity, and this is further exacerbated when mice are fed a high-fat diet. Additionally, we demonstrate that PP is an endogenous high-affinity ligand for *Npy6r* in mice, since exogenous administration of PP, but not PYY or PYY3-36, activated *Npy6r*-expressing neurons in the SCN, and this effect was absent in *Npy6r*-deficient mice. The mechanism by which *Npy6r* mediates its effects on the GH axis and energy homeostasis is most likely through alterations in VIP signaling in the hypothalamus. This is demonstrated by the strong overlap in expression of *Vip* and *Npy6r* within the SCN, the brain region to which the *Npy6r* is confined, and the significant reduction in *Vip* expression in this nucleus in the absence of *Npy6r* signaling. Moreover, the fact that i.p. PP injection increases energy expenditure and decreases food intake, hypothalamic *Ghrh* mRNA expression, and circulating IGF-1 levels in WT but not in *Npy6r*$^{-/-}$ mice, and that the effect on IGF-1 is blocked by prior administration of a VPAC receptors antagonist, strongly supports this stand.

It has been documented that the SCN contains the master circadian clock in mammals; it generates distinct temporal changes in biological processes such as core body temperature and hormone secretion (Huang et al., 2011). Disruptions in circadian rhythm, whether by genetic or environmental influences, can result in metabolic dysfunction (Huang et al., 2011). For instance, mutation of either of two key regulators of the circadian cycle, circadian locomotor output cycles kaput (CLOCK) or brain and muscle aryl hydrocarbon receptor nuclear translocator (ARNT)-like 1 (BMAL1), not only disrupt normal circadian rhythm, manifesting in loss of normal daily hormonal and feeding patterns, but also predispose mice to metabolic diseases (Marcheva et al., 2010; Rudic et al., 2004; Turek et al., 2005). VIP is a critical regulator of circadian rhythm in the SCN, with deletion of VIP or its receptor, VPAC2, leading to loss of circadian rhythmicity and synchrony in SCN neurons (Aton et al., 2005; Hannibal et al., 2011; Harmar et al., 2004). Since our studies demonstrate that hypothalamic VIP expression is reduced in *Npy6r*-deficient mice, it is possible that the impaired circadian rhythm observed in our *Npy6r*$^{-/-}$ mice, as evidenced by blunted daily fluctuations in serum corticosterone levels and reduced light-phase feeding, may be due to impaired VIP signaling, and therefore could contribute to the development of metabolic abnormalities in these mice.

In addition to regulating circadian rhythm, VIP is an important regulator of the GH axis. VIP is known to stimulate GH release in rats in vivo (Bluet-Pajot et al., 1987), in cultured bovine adenohypophysial cells (Soliman et al., 1995), and in perifused bovine adenohypophysis (Hashizume and Kanematsu, 1990). Moreover, loss of VIP or VPAC2 in mice leads to reduced growth in association with reduced circulating IGF-1 levels (Asnicar et al., 2002; Niewiadomski et al., 2008). Indeed, we demonstrate that blockade of VPAC abolishes the *Npy6r*-mediated alteration of circulating IGF-1 levels. This finding, combined with our observations of reduced SCN *Vip* mRNA expression and reduced GH/IGF-1 axis activity in our *Npy6r*$^{-/-}$ mice, suggests that the reduced lean mass and late onset obesity observed in the absence of *Npy6r* signaling are due to perturbations in normal VIP regulation of the GH/IGF-1 axis. Consistent with known effects of reduced circulating IGF-1 levels in inducing obesity (Rosen et al., 2004), our data suggest that the lower circulating IGF-1 levels could account for the decreased lean mass and the increased relative adiposity in *Npy6r*$^{-/-}$ mice. Thus, impairment in function of the GH/IGF-1 axis, as well as impaired circadian rhythmicity resulting from defects in VIP neuronal signaling pathways in the SCN, could have contributed to the reduction in lean body mass and the development of late-onset obesity in *Npy6r*$^{-/-}$ mice.

In this study, PP was found to be the only high-affinity ligand that can trigger significant elevation of Fos expression in the SCN in WT compared to *Npy6r*$^{-/-}$ mice. PP is released from pancreatic F cells in response to stimuli such as food intake and hypoglycemia, mainly by vagal muscarinic activation (Havel et al., 1993). Previously it was thought to be a ligand only for the *Ppyr1*, triggering responses in the brain stem and ARC to inhibit food intake (Lin et al., 2009) and enhance digestive events such as gastric secretion, motility, and emptying by subsequent activation of vagal cholinergic pathways (McTigue et al., 1997). Lack

Figure 7. Pancreatic Polypeptide-Mediated Npy6r Signaling Controls VIP Expression in the SCN

(A–C) (A) *Vip* mRNA expression in the hypothalamus and (B and C) in SCN of *Npy6r*$^{-/-}$ mice and WT controls.

(D and E) Fasted serum IGF-1 and hypothalamic *Ghrh* mRNA expression were determined in chow-fed *Npy6r*$^{-/-}$ and WT mice.

(F and G) Serum corticosterone levels were assessed at intervals of 6 hr or under fasted condition in *Npy6r*$^{-/-}$ mice and WT controls.

(H and I) Light- and dark-phase food intake was measured for 6 consecutive days in 16- and 23-week-old *Npy6r*$^{-/-}$ and WT mice.

(J and K) *Npy6r*$^{-/-}$ and WT mice were injected with either saline or PP, and *Ghrh* mRNA levels in ARC were assessed.

(L) *Npy6r*$^{-/-}$ and WT mice were injected with either saline, PP, or PP and VIP receptor antagonist. Subsequently, serum IGF-1 levels were determined by using IGF-1 ELISA kit. Data are means ±SEM of four to eight mice per group. See also Figure S7.

of *Ppyr1* signaling in mice leads to reduced body weight and fat mass on a lean background, and attenuation of certain aspects of the obesity syndrome and enhanced fertility on a background of leptin deficiency (Sainsbury et al., 2002b; Zhang et al., 2010). However, satiety regulation of PP via *Ppyr1* signaling seems to be mainly confined to the ARC in the hypothalamus, particularly to neurons that coexpress alpha melanocyte stimulating hormone (α-MSH) (Lin et al., 2009). It is possible that the reduced body weight or attenuated obesity syndrome of *Ppyr1*$^{-/-}$ mice was mediated by the high circulating PP concentrations seen in these mice, acting on other Y receptors besides *Ppyr1*, such as the herein-identified *Npy6r*. In support of this, PP transgenic mice, which have a 20-fold increase in plasma PP levels, have a similar metabolic phenotype to *Ppyr1*$^{-/-}$ mice (Ueno et al., 1999). Our current data extend these findings to suggest that the late-onset obesity phenotype of our *Npy6r*$^{-/-}$ mice could be mediated by lack of action of PP on Npy6r in the SCN.

In summary, our study demonstrates that *Npy6r* is a critical regulator of energy homeostasis and body composition, with germline deletion of *Npy6r* leading to reduced body weight, inhibition of lean body mass, and an age-dependent increase in adiposity that is exacerbated by high-fat feeding, with these effects likely mediated via the lack of Npy6r signaling in the SCN to influence the VIP-GH/IGF-1 axis. Future studies in mice into the function and possible clinical utility of Y receptors and their ligands as drug targets must therefore take into account this new knowledge that *Npy6r* plays an important role in the regulation of energy homeostasis.

EXPERIMENTAL PROCEDURES

Animals

All animal care and experiments were approved by the Garvan/St. Vincent's Animal Ethics Committee. *Npy6r*$^{-/-}$ mice were generated and genotyped as described in Supplemental Experimental Procedures. Male mice on a mixed C57BL/6–129SvJ background were used for all experiments, except where noted. Mice were housed under a controlled temperature of 22°C and a 12 hr light cycle (lights on from 07:00 to 19:00 hr) with ad libitum access to water and a standard chow diet (6% calories from fat, 21% calories from protein, 71% calories from carbohydrate, 2.6 kcal/g, Gordon's Specialty Stock Feeds, Australia) or fed a HFD (43% kilojoules from fat, 17% kilojoules from protein, 40% kilojoules from carbohydrate, 4.8 kcal/g, Specialty Feeds, Australia) for 16 weeks starting from 7–8 weeks of age.

RNA Extraction and Quantitative Real-Time PCR

Hypothalami were dissected and immediately frozen in liquid N_2, and RNA was extracted using Trizol Reagent (Sigma, St. Louis, MO) and processed for quantitative real-time PCR with the Light-Cycler 480 Real-Time PCR system (Roche, Switzerland) as described in the Supplemental Experimental Procedures.

Metabolic Measurements and Body Composition

Weekly body weight was determined from 6 weeks of age onward, unless otherwise stated. Food intake and fecal output were examined in chow- and high-fat-fed mice under normal and fasting states as described in the Supplemental Experimental Procedures. Whole-body lean and fat masses were determined by DXA (Lunar Piximus II mouse densitometer; GE Healthcare, UK) as previously described (Baldock et al., 2009; Zhang et al., 2010). VO_2, energy expenditure, RER, and physical activity were assessed using an indirect calorimeter (Oxymax series; Columbus Instruments, Columbus, OH) as described in the Supplemental Experimental Procedures.

Glucose Tolerance Tests and Serum Assays

Mice were fasted for 16–18 hr and i.p. administered with glucose (1 mg/kg body weight). Blood glucose levels were assessed at 0, 15, 30, 60, and 90 min after glucose administration using an Accu-chek Go glucometer (Roche, Dee Why, Australia). Serum was collected and stored for subsequent insulin assay. Serum insulin, testosterone, IGF-1, VIP, and corticosterone levels were measured in accordance with the manufacturers' specifications as described in the Supplemental Experimental Procedures.

Oil Red O and β-Galactosidase Staining

Frozen livers sections (6 μm) were cut on a cryostat, mounted on slides, and processed for oil red O staining as described in the Supplemental Experimental Procedures. Coronal brain and peripheral tissue frozen sections (25 μm) were mounted on slides and processed for β-galactosidase histochemistry as described in the Supplemental Experimental Procedures.

Immunohistochemistry

Animals were anesthetized, and the brains were perfused with saline and then 4% paraformaldehyde (PFA). Brains were postfixed in 4% PFA, then placed in 30% sucrose overnight and cut at 35 μm on a cryostat. Subsequently, immunohistochemistry was performed using antibodies against Fos, p-ERK, VIP, or AVP. Fos expression was visualized in brain sections containing the SCN (Bregma −0.34 mm through to −0.70 mm) (Franklin and Paxinos, 1997) with a light microscope (Leica, Heerbrugg, Switzerland). The number of Fos-positive neurons within a constant and defined frame was counted using ImageJ64 software (National Institutes of Health).

In Situ Hybridization and Colocalization Study

Coronal brain sections (30 μm) were cut on a cryostat and mounted on slides. Matching sections from the same coronal brain level from different groups of mice were examined together using radiolabeled DNA oligonucleotides complementary to mouse Vip and Ghrh. Sequence of probes and details of the in situ hydridization methodology can be found in the Supplemental Experimental Procedures. For colocalization of *Npy6r* and *Vip* study, coronal brain section were first processed for β-gal staining, then followed by in situ hydridization as described in the Supplemental Experimental Procedures. Slides were visualized and imaged with a light microscope (Leica, Heerbrugg, Switzerland).

Stereotaxic Brain Delivery of Peptides

Adult mice were anaesthetized and placed on a Kopf stereotaxic frame (David Kopf Instruments, Tujunga, CA, USA). A total of 1 μl PP or 1.5 μl VPAC2 antagonist (2 μg/ul) was injected into the lateral ventricle at a rate of 0.1 μL/min using a 10 μl Hamilton syringe attached to Micro4 Micro Syringe Pump Controller (World Precision Instruments Inc., Sarasota). The injection coordinates were (from bregma) as follows: anteroposterior, –0.34 mm; mediolateral, ±1.00 mm; and dorsoventral, –2.5 mm (Franklin and Paxinos, 1997). Animals were kept on a heating pad during surgery.

Statistical Analyses

All data are expressed as mean ±SEM. A two-tailed Student's t test was used to test the difference between two groups of mice. Differences among groups of mice were assessed by two-way ANOVA or repeated-measures ANOVA. Bonferroni post hoc tests were performed to identify differences among means. Statistical analyses were assessed using Prism software (GraphPad Software, Inc, LaJolla). Differences were regarded as statistically significant if $p < 0.05$.

SUPPLEMENTAL INFORMATION

Supplemental Information includes seven figures, two tables, and Supplemental Experimental Procedures and can be found with this article at http://dx.doi.org/10.1016/j.cmet.2013.11.019.

ACKNOWLEDGMENTS

This work was supported by the National Health and Medical Research Council (NHMRC) of Australia in the form of a Postgraduate Scholarship to

E.Y., a Fellowship to H.H., a Senior Research Fellowship to A.S., and project grant #427661 to H.H. and A.S. We thank Dr. Hal Gainer from the National Institute of Neurological Disorders and Stroke for his gifts of antibodies. We are grateful to Dr Robert Dallmann, Nguyen Dinh Nguyen, and Andrea Abdipranoto for their helpful discussions. We thank Felicity Forsyth for secretarial assistance.

Received: October 29, 2012
Revised: October 4, 2013
Accepted: November 15, 2013
Published: January 7, 2014

REFERENCES

Asnicar, M.A., Köster, A., Heiman, M.L., Tinsley, F., Smith, D.P., Galbreath, E., Fox, N., Ma, Y.L., Blum, W.F., and Hsiung, H.M. (2002). Vasoactive intestinal polypeptide/pituitary adenylate cyclase-activating peptide receptor 2 deficiency in mice results in growth retardation and increased basal metabolic rate. Endocrinology *143*, 3994–4006.

Aton, S.J., Colwell, C.S., Harmar, A.J., Waschek, J., and Herzog, E.D. (2005). Vasoactive intestinal polypeptide mediates circadian rhythmicity and synchrony in mammalian clock neurons. Nat. Neurosci. *8*, 476–483.

Baldock, P.A., Lee, N.J., Driessler, F., Lin, S., Allison, S., Stehrer, B., Lin, E.J., Zhang, L., Enriquez, R.F., Wong, I.P., et al. (2009). Neuropeptide Y knockout mice reveal a central role of NPY in the coordination of bone mass to body weight. PLoS ONE *4*, e8415.

Bechtold, D.A., Brown, T.M., Luckman, S.M., and Piggins, H.D. (2008). Metabolic rhythm abnormalities in mice lacking VIP-VPAC2 signaling. Am. J. Physiol. Regul. Integr. Comp. Physiol. *294*, R344–R351.

Bluet-Pajot, M.T., Mounier, F., Leonard, J.F., Kordon, C., and Durand, D. (1987). Vasoactive intestinal peptide induces a transient release of growth hormone in the rat. Peptides *8*, 35–38.

Brown, T.M., Colwell, C.S., Waschek, J.A., and Piggins, H.D. (2007). Disrupted neuronal activity rhythms in the suprachiasmatic nuclei of vasoactive intestinal polypeptide-deficient mice. J. Neurophysiol. *97*, 2553–2558.

Burkhoff, A., Linemeyer, D.L., and Salon, J.A. (1998). Distribution of a novel hypothalamic neuropeptide Y receptor gene and it's absence in rat. Brain Res. Mol. Brain Res. *53*, 311–316.

Dulloo, A.G. (2009). Adipose tissue plasticity in catch-up-growth trajectories to metabolic syndrome: hyperplastic versus hypertrophic catch-up fat. Diabetes *58*, 1037–1039.

Franklin, K.B.J., and Paxinos, G. (1997). The Mouse Brain in Stereotaxic Coordinates. (San Diego: Academic Press).

Gregor, P., Feng, Y., DeCarr, L.B., Cornfield, L.J., and McCaleb, M.L. (1996). Molecular characterization of a second mouse pancreatic polypeptide receptor and its inactivated human homologue. J. Biol. Chem. *271*, 27776–27781.

Hannibal, J., Hsiung, H.M., and Fahrenkrug, J. (2011). Temporal phasing of locomotor activity, heart rate rhythmicity, and core body temperature is disrupted in VIP receptor 2-deficient mice. Am. J. Physiol. Regul. Integr. Comp. Physiol. *300*, R519–R530.

Harmar, A.J., Sheward, W.J., Morrison, C.F., Waser, B., Gugger, M., and Reubi, J.C. (2004). Distribution of the VPAC2 receptor in peripheral tissues of the mouse. Endocrinology *145*, 1203–1210.

Hashizume, T., and Kanematsu, S. (1990). Effects of VIP and GRF on the release of growth hormone in perifused bovine adenohypophysis. Domest. Anim. Endocrinol. *7*, 451–456.

Havel, P.J., Akpan, J.O., Curry, D.L., Stern, J.S., Gingerich, R.L., and Ahren, B. (1993). Autonomic control of pancreatic polypeptide and glucagon secretion during neuroglucopenia and hypoglycemia in mice. Am. J. Physiol. *265*, R246–R254.

Huang, W., Ramsey, K.M., Marcheva, B., and Bass, J. (2011). Circadian rhythms, sleep, and metabolism. J. Clin. Invest. *121*, 2133–2141.

Lichanska, A.M., and Waters, M.J. (2008). How growth hormone controls growth, obesity and sexual dimorphism. Trends Genet. *24*, 41–47.

Lin, S., Shi, Y.C., Yulyaningsih, E., Aljanova, A., Zhang, L., Macia, L., Nguyen, A.D., Lin, E.J., During, M.J., Herzog, H., and Sainsbury, A. (2009). Critical role of arcuate Y4 receptors and the melanocortin system in pancreatic polypeptide-induced reduction in food intake in mice. PLoS ONE *4*, e8488.

Loh, D.H., Abad, C., Colwell, C.S., and Waschek, J.A. (2008). Vasoactive intestinal peptide is critical for circadian regulation of glucocorticoids. Neuroendocrinology *88*, 246–255.

Marcheva, B., Ramsey, K.M., Buhr, E.D., Kobayashi, Y., Su, H., Ko, C.H., Ivanova, G., Omura, C., Mo, S., Vitaterna, M.H., et al. (2010). Disruption of the clock components CLOCK and BMAL1 leads to hypoinsulinaemia and diabetes. Nature *466*, 627–631.

Marra, M., Scalfi, L., Contaldo, F., and Pasanisi, F. (2004). Fasting respiratory quotient as a predictor of long-term weight changes in non-obese women. Ann. Nutr. Metab. *48*, 189–192.

Matsumoto, M., Nomura, T., Momose, K., Ikeda, Y., Kondou, Y., Akiho, H., Togami, J., Kimura, Y., Okada, M., and Yamaguchi, T. (1996). Inactivation of a novel neuropeptide Y/peptide YY receptor gene in primate species. J. Biol. Chem. *271*, 27217–27220.

McTigue, D.M., Hermann, G.E., and Rogers, R.C. (1997). Effect of pancreatic polypeptide on rat dorsal vagal complex neurons. J. Physiol. *499*, 475–483.

Mullins, D.E., Guzzi, M., Xia, L., and Parker, E.M. (2000). Pharmacological characterization of the cloned neuropeptide Y y(6) receptor. Eur. J. Pharmacol. *395*, 87–93.

Nakamura, M., Sakanaka, C., Aoki, Y., Ogasawara, H., Tsuji, T., Kodama, H., Matsumoto, T., Shimizu, T., and Noma, M. (1995). Identification of two isoforms of mouse neuropeptide Y-Y1 receptor generated by alternative splicing. Isolation, genomic structure, and functional expression of the receptors. J. Biol. Chem. *270*, 30102–30110.

Nettleship, J.E., Jones, T.H., Channer, K.S., and Jones, R.D. (2007). Physiological testosterone replacement therapy attenuates fatty streak formation and improves high-density lipoprotein cholesterol in the Tfm mouse: an effect that is independent of the classic androgen receptor. Circulation *116*, 2427–2434.

Nguyen, A.D., Herzog, H., and Sainsbury, A. (2011). Neuropeptide Y and peptide YY: important regulators of energy metabolism. Curr. Opin. Endocrinol. Diabetes Obes. *18*, 56–60.

Nguyen, A.D., Mitchell, N.F., Lin, S., Macia, L., Yulyaningsih, E., Baldock, P.A., Enriquez, R.F., Zhang, L., Shi, Y.C., Zolotukhin, S., et al. (2012). Y1 and Y5 receptors are both required for the regulation of food intake and energy homeostasis in mice. PLoS ONE *7*, e40191.

Niewiadomski, P., Coute-Monvoisin, A.C., Abad, C., Ngo, D., Menezes, A., and Waschek, J.A. (2008). Mice deficient in both pituitary adenylyl cyclase-activating polypeptide and vasoactive intestinal peptide survive, but display growth retardation and sex-dependent early death. J. Mol. Neurosci. *36*, 200–207.

Pantazopoulos, H., Dolatshad, H., and Davis, F.C. (2010). Chronic stimulation of the hypothalamic vasoactive intestinal peptide receptor lengthens circadian period in mice and hamsters. Am. J. Physiol. Regul. Integr. Comp. Physiol. *299*, R379–R385.

Piggins, H.D., and Cutler, D.J. (2003). The roles of vasoactive intestinal polypeptide in the mammalian circadian clock. J. Endocrinol. *177*, 7–15.

Reghunandanan, V., Reghunandanan, R., and Singh, P.I. (1993). Neurotransmitters of the suprachiasmatic nucleus: role in the regulation of circadian rhythms. Prog. Neurobiol. *41*, 647–655.

Rose, P.M., Lynch, J.S., Frazier, S.T., Fisher, S.M., Chung, W., Battaglino, P., Fathi, Z., Leibel, R., and Fernandes, P. (1997). Molecular genetic analysis of a human neuropeptide Y receptor. The human homolog of the murine "Y5" receptor may be a pseudogene. J. Biol. Chem. *272*, 3622–3627.

Rosen, C.J., Ackert-Bicknell, C.L., Adamo, M.L., Shultz, K.L., Rubin, J., Donahue, L.R., Horton, L.G., Delahunty, K.M., Beamer, W.G., Sipos, J., et al. (2004). Congenic mice with low serum IGF-I have increased body fat, reduced bone mineral density, and an altered osteoblast differentiation program. Bone *35*, 1046–1058.

Rudic, R.D., McNamara, P., Curtis, A.M., Boston, R.C., Panda, S., Hogenesch, J.B., and Fitzgerald, G.A. (2004). BMAL1 and CLOCK, two essential components of the circadian clock, are involved in glucose homeostasis. PLoS Biol. *2*, e377.

Sainsbury, A., Cooney, G.J., and Herzog, H. (2002a). Hypothalamic regulation of energy homeostasis. Best Pract. Res. Clin. Endocrinol. Metab. *16*, 623–637.

Sainsbury, A., Schwarzer, C., Couzens, M., Jenkins, A., Oakes, S.R., Ormandy, C.J., and Herzog, H. (2002b). Y4 receptor knockout rescues fertility in ob/ob mice. Genes Dev. *16*, 1077–1088.

Sattler, F.R., Castaneda-Sceppa, C., Binder, E.F., Schroeder, E.T., Wang, Y., Bhasin, S., Kawakubo, M., Stewart, Y., Yarasheski, K.E., Ulloor, J., et al. (2009). Testosterone and growth hormone improve body composition and muscle performance in older men. J. Clin. Endocrinol. Metab. *94*, 1991–2001.

Schutz, Y. (2004). Concept of fat balance in human obesity revisited with particular reference to de novo lipogenesis. Int. J. Obes. Relat. Metab. Disord. *28* (*Suppl 4*), S3–S11.

Seidell, J.C., Muller, D.C., Sorkin, J.D., and Andres, R. (1992). Fasting respiratory exchange ratio and resting metabolic rate as predictors of weight gain: the Baltimore Longitudinal Study on Aging. Int. J. Obes. Relat. Metab. Disord. *16*, 667–674.

Sheward, W.J., Maywood, E.S., French, K.L., Horn, J.M., Hastings, M.H., Seckl, J.R., Holmes, M.C., and Harmar, A.J. (2007). Entrainment to feeding but not to light: circadian phenotype of VPAC2 receptor-null mice. J. Neurosci. *27*, 4351–4358.

Shi, Y.C., Lin, S., Wong, I.P., Baldock, P.A., Aljanova, A., Enriquez, R.F., Castillo, L., Mitchell, N.F., Ye, J.M., Zhang, L., et al. (2010). NPY neuron-specific Y2 receptors regulate adipose tissue and trabecular bone but not cortical bone homeostasis in mice. PLoS ONE *5*, e11361.

Shi, Y.C., Lin, Z., Lau, J., Zhang, H., Yagi, M., Kanzler, I., Sainsbury, A., Herzog, H., and Lin, S. (2013). PYY3-36 and pancreatic polypeptide reduce food intake in an additive manner via distinct hypothalamic dependent pathways in mice. Obesity (Silver Spring). Published online June 26, 2013. http://dx.doi.org/10.1002/oby.20534.

Soliman, E.B., Hashizume, T., Ohashi, S., and Kanematsu, S. (1995). The interactive effects of VIP, PHI, GHRH, and SRIF on the release of growth hormone from cultured adenohypophysial cells in cattle. Endocr. J. *42*, 717–722.

Turek, F.W., Joshu, C., Kohsaka, A., Lin, E., Ivanova, G., McDearmon, E., Laposky, A., Losee-Olson, S., Easton, A., Jensen, D.R., et al. (2005). Obesity and metabolic syndrome in circadian Clock mutant mice. Science *308*, 1043–1045.

Ueno, N., Inui, A., Iwamoto, M., Kaga, T., Asakawa, A., Okita, M., Fujimiya, M., Nakajima, Y., Ohmoto, Y., Ohnaka, M., et al. (1999). Decreased food intake and body weight in pancreatic polypeptide-overexpressing mice. Gastroenterology *117*, 1427–1432.

Weinberg, D.H., Sirinathsinghji, D.J., Tan, C.P., Shiao, L.L., Morin, N., Rigby, M.R., Heavens, R.H., Rapoport, D.R., Bayne, M.L., Cascieri, M.A., et al. (1996). Cloning and expression of a novel neuropeptide Y receptor. J. Biol. Chem. *271*, 16435–16438.

Weinsier, R.L., Nelson, K.M., Hensrud, D.D., Darnell, B.E., Hunter, G.R., and Schutz, Y. (1995). Metabolic predictors of obesity. Contribution of resting energy expenditure, thermic effect of food, and fuel utilization to four-year weight gain of post-obese and never-obese women. J. Clin. Invest. *95*, 980–985.

Welsh, D.K., Takahashi, J.S., and Kay, S.A. (2010). Suprachiasmatic nucleus: cell autonomy and network properties. Annu. Rev. Physiol. *72*, 551–577.

Zhang, L., Riepler, S.J., Turner, N., Enriquez, R.F., Lee, I.C., Baldock, P.A., Herzog, H., and Sainsbury, A. (2010). Y2 and Y4 receptor signaling synergistically act on energy expenditure and physical activity. Am. J. Physiol. Regul. Integr. Comp. Physiol. *299*, R1618–R1628.

Zhang, L., Bijker, M.S., and Herzog, H. (2011). The neuropeptide Y system: pathophysiological and therapeutic implications in obesity and cancer. Pharmacol. Ther. *131*, 91–113.